Time-division multiplexing holographic display using angular-spectrum layer-oriented method

(Invited Paper)

Yan Zhao (赵 燕), Liangcai Cao (曹良才)*, Hao Zhang (张 浩), Wei Tan (谭 巍), Shenghan Wu (吴圣涵), Zheng Wang (王 峭), Qiang Yang (杨 强), and Guofan Jin (金国藩)

State Key Laboratory of Precision Measurement Technology and Instruments, Department of Precision Instruments, Tsinghua University, Beijing 100084, China

**Corresponding author: clc@tsinghua.edu.cn*

Received September 15, 2015; accepted October 27, 2015; posted online December 14, 2015

A time-division multiplexing method for computer-generated holograms (CGHs) is proposed to solve the problem of the limited space-bandwidth product. A three-dimensional (3-D) scene is divided into multiple layers at different depths. The CGH corresponding to each layer is calculated by an angular-spectrum algorithm that is effective at a wide range of propagation distances. All of the CGHs are combined into several group-CGHs. These group-CGHs are sequentially uploaded onto one spatial light modulator at a high frame rate. The space-bandwidth product can be benefited by the time-division processing of the CGHs. The proposed method provides a new approach to achieve high quality 3-D display with a fast and accurate CGH computation.

OCIS codes: 090.0090, 090.1760, 090.2870.

doi: 10.3788/COL201614.010005.

Holography is a promising way for displaying three-dimensional (3-D) images since it can reconstruct the whole optical wave field of the 3-D scene and has the potential to provide all of the depth cues that human eyes can perceive[1]. For electronic holographic display, the computer-generated holograms (CGHs) can be synthesized without complicated interference recording systems. As long as the mathematical description of the 3-D data is provided, it could be encoded in a CGH and then reconstructed for display. With the developments of spatial light modulators (SLMs) and computing techniques, the CGHs can be displayed in real time[2,3].

The space-bandwidth product (SBP) of the hologram determines the optical performance of the holographic display system. Holograms recorded in photosensitive materials can provide enough SBP to reconstruct high-quality 3-D images. In contrast, the CGH systems have a pixelated structure with finite pixel numbers and micrometer-scaled pixel size that are limited by the manufacturing technology of commercially available SLM, leading to a much lower SBP. This limitation bottlenecks the applications of CGH systems. Many works have been done for better optical performance by spatially expanding the CGH system's SBP[4–10]. These spatial multiplexing techniques effectively increased the image resolution and the field of view (FOV).

With the developments of high-speed SLMs, time-multiplexing techniques were proposed to reduce speckles in the reconstructed images[11] and improve the optical performances of the holographic display systems by expanding their SBPs[12–14].

Apart from the display devices, the algorithm of CGH is another important factor for the holographic display system. It is directly related to the quality of the reconstructed image and the computing speed. Major CGH algorithms are physically-based, including point-oriented[15–17] and polygon-oriented algorithms[18–20], which can provide precise geometrical information of the 3-D scene. However, since the amount of the primitives would be extremely large for reconstructing a complicated 3-D scene, the computational load would also be increased drastically. In order to accelerate the computing speed, several layer-based approaches using Fresnel diffraction algorithms were proposed[21–23]. However, the paraxial approximation of the Fresnel diffraction algorithms will reduce the fidelity of reconstructed images in high numerical aperture (NA) systems.

In this study, a time-division multiplexing method with an angular-spectrum algorithm is proposed. Different from the scanning-based time multiplexing method, the CGHs are generated from layers at different depths of the 3-D scene and uploaded on the SLM sequentially. The 3-D scene is divided into multiple groups according to their depth information. One group of 3-D scenes is contributed by one CGH and its optical information is reconstructed by all of the hologram samples. By refreshing the segmented CGHs as required by the human vision system, the entire 3-D scene can be perceived without flicker artifacts. The proposed method can improve the display quality and reduce the problem of the limited SBP. To match the speed of the proposed time-division method, the angular-spectrum layer-oriented algorithm is implemented to accelerate the generation of the CGH according to the depth information of the 3-D scene, without using paraxial approximation[24]. Numerical simulations and optical experiments for both

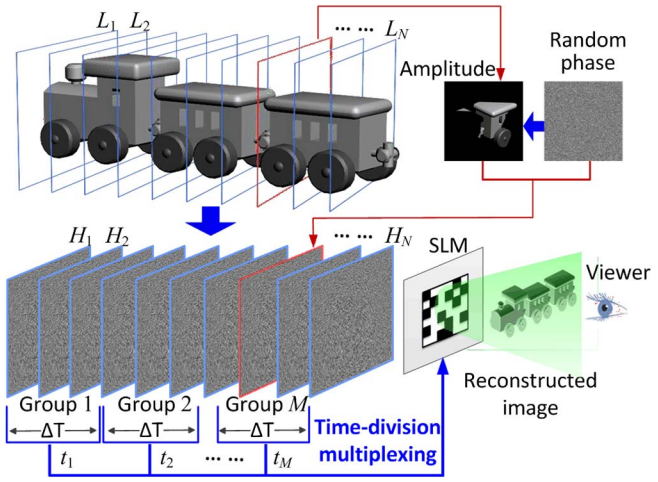

Fig. 1. CGH calculation process and the image reconstruction process of the time-division multiplexing method.

two-dimensional (2-D) images and 3-D scenes are performed. The results show that high-quality images can be reconstructed by using the proposed method.

The CGH calculation process and the image reconstruction process are shown in Fig. 1. The 3-D scene is decomposed into multiple 2-D layers with a uniform layer interval. A layer-CGH corresponding to each layer is calculated in the plane of the hologram, respectively. All of the layer-CGHs can be summed up as one final CGH for the 3-D scene in the traditional method. In the time-division multiplexing method, all of the layers are divided into several groups. The CGHs of the layers in each group are summed up and one group-CGH is acquired. All of the group-CGHs are uploaded on the high-speed SLM sequentially. The whole 3-D scene can be smoothly observed based on the persistence of human vision. The SBP of the display system is fully utilized because one superimposed CGH for a complicated 3-D scene is decomposed into several group-CGHs. The information capacity presented by one SLM device can be increased multiple times using the method of temporal multiplexing. Since the refresh rate of both the liquid-crystal-based SLM (e.g., LCoS) and the digital micromirror device-based SLM (e.g., DMD) can be from 60 to more than 1000 frames per second, it is possible to enhance the display resolution at the cost of the time accumulation of multiple subframes based on current devices.

The display quality is mainly determined by the calculation algorithm of the CGHs. The proposed time-division multiplexing method consists of four steps. At the first step, a computer graphics rendering technique is employed to slice the complex 3-D scene into multiple layers with depth cues along the directional normal to the plane of the hologram. The distance intervals between the layers and the number of the layers are carefully selected to sample the 3-D scene. The 3-D scene is sliced into N layers, $L_1, L_2, \ldots L_i, \ldots, L_N$. The 3-D scene located within L_i and L_{i+1} is encoded in the shading image of L_i with the corresponding propagation distance according to the depth map. The image for the ith layer can be written as a complex amplitude distribution,

$$L_i(\xi,\eta) = A_i(\xi,\eta)\exp[j\phi_i(\xi,\eta)], \tag{1}$$

where (ξ,η) is the coordinate system of the ith layer, $A_i(\xi,\eta)$ is the amplitude distribution of the ith layer that can be extracted from its shading image, and $\phi_i(\xi,\eta)$ is the random phase distribution which simulates the diffusive 3-D object. At the second step, based on the complex amplitude distributions of the sliced layers, the angular-spectrum propagation method is employed to calculate the CGHs of all of the parallel layer images at the distances between the layers and the hologram. The complex amplitude distribution of the ith hologram H_i corresponding to the ith layer is calculated by the angular-spectrum method[25] using

$$H_i(x,y) = \mathcal{F}^{-1}\{H_F(f_\xi,f_\eta)\mathcal{F}[L_i(\xi,\eta)]\}, \tag{2}$$

where H_F is the angular-spectrum transfer function, and $\mathcal{F}$ and $\mathcal{F}^{-1}$ denote the Fourier and the inverse Fourier transforms, respectively. The transfer function from the ith layer to the hologram plane is

$$H_F(f_\xi,f_\eta) = \exp\left(jkz\sqrt{1-\lambda^2 f_\xi^2-\lambda^2 f_\eta^2}\right), \tag{3}$$

where (f_ξ, f_η) are spatial frequencies, $k = 2\pi/\lambda$ is the wavenumber, and z is the propagation distance. Thus N layer-CGHs, $H_1, H_2, \ldots H_i, \ldots, H_N$, are acquired. In the third step, all of the N layer-CGHs are combined into M groups according to a predetermined rule. Each group consists of N/M layer-CGHs and each group-CGH is acquired by summing up the N/M layer-CGHs. By summing up the layer-CGHs in a certain group, the complex distribution of the hologram of the mth group can be calculated,

$$H_m(x,y) = \sum_{i=m_1}^{m_k} H_i(x,y). \tag{4}$$

Then, we discard the amplitude information of the group-CGH and keep the phase information only. Now we have M phase-only group-CGHs ready for uploading. At the last step, the group-CGHs are uploaded on a phase-only SLM sequentially. When the group-CGH 1 which is related to the group 1 of the 3-D scene is loaded, the viewing of group 1 can be viewed by the eyes. Likewise, the group-CGH 2 and group-CGH 3 are sequentially loaded on for viewing group 2 and 3. These M subframes can be united into a frame of the whole 3-D scene using the time-division multiplexing method, as shown in Fig. 1.

The comparison between the angular-spectrum and Fresnel diffraction algorithm at different propagation distances is shown in Fig. 2. A simple image containing one letter "H" is shown in Fig. 2(a) with sampling number 1920×1920 and sampling distance 8 μm. By using the angular-spectrum algorithm, we may have the high-quality reconstructions at different distances. However, by using the Fresnel diffraction algorithm, the quality of the reconstructions is reduced seriously at the short distances.

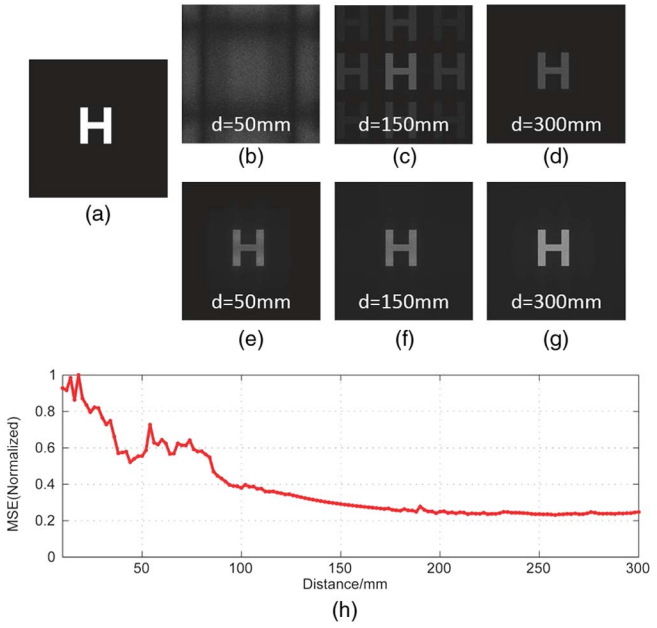

Fig. 2. (a) Original image of the letter "H". (b), (c), and (d) are the reconstructed images at the distances of 50, 150, and 300 mm between the layer and the CGH plane when using the Fresnel diffraction algorithm. (e), (f), and (g) are the reconstructed images at the corresponding propagation distances when using the angular-spectrum algorithm. (h) The MSE curve of the reconstructions between the angular-spectrum algorithm and the Fresnel diffraction algorithm at different distances.

The reconstructed images at $d = 50$, 150, and 300 mm are presented in Figs. 2(b)–2(d). It could be seen that when $d = 50$ mm, the reconstruction of the letter "H" cannot be recognized. While the reconstructed images at the corresponding propagation distances when using the angular-spectrum algorithm are shown in Figs. 2(e)–2(g). To evaluate the reconstruction quality, the CGH at the distance interval of 2 mm by using the angular-spectrum and Fresnel diffraction algorithms are calculated, respectively. Then, we compare the reconstructed images by use of the mean squared error (MSE) value. As is shown in Fig. 2(h), when the propagation distance is larger than 150 mm, the MSE value is low enough and the reconstructions with these two algorithms are of the same level. When the distance is less than 150 mm, the MSE value becomes high. Due to the paraxial approximation of the Fresnel diffraction algorithm, the calculation error would be more serious in high NA systems. A high NA system is preferred in holographic 3-D displays to produce better viewing parameters, and the angular-spectrum method can produce accurate calculations for these kinds of applications[24].

To demonstrate the feasibility of the proposed method, we implement the algorithm in numerical simulations and optical experiments by using a 3-D digital train model and letters at different depths. The train model is sliced into 51 layers, which are then divided into 3 groups. The phase distributions of the group-CGHs are extracted for optical reconstruction. Then, the group-CGHs are uploaded on the phase-only SLM sequentially at a rate of 60 Hz.

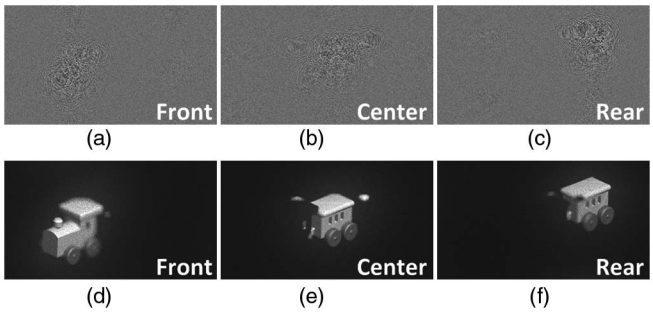

Fig. 3. Numerical reconstructions of the 3-D scene of a train model. (a) The group-CGH 1 of the train, (b) the group-CGH 2 of the train. (c) the group-CGH 3 of the train, (d) the numerical reconstruction of the group-CGH 1, (e) the numerical reconstruction of the group-CGH 2, and (f) the numerical reconstruction of the group-CGH 3.

Figure 3 shows the numerical simulations of the train model. Figures 3(a)–3(c) are the holograms of the front, center, and rear part of the train, respectively. Figures 3(d)–3(f) are numerical reconstructions of the three group-CGHs. According to the time sequence for the group-CGHs, multiple reconstruction zones at multiple depths are created. To meet the requirements for eyes, we utilize the real-time control system of the SLM. Each reconstruction zone uses 1/60 s to display one group-CGH. The CGHs are grouped corresponding to each part of the 3-D scene. For the three reconstruction zones, each zone has 17 layers. The three groups of holograms are sequentially loaded at a rate of 60 Hz. Generally, each reconstruction zone equally shares 1/60 s for one hologram

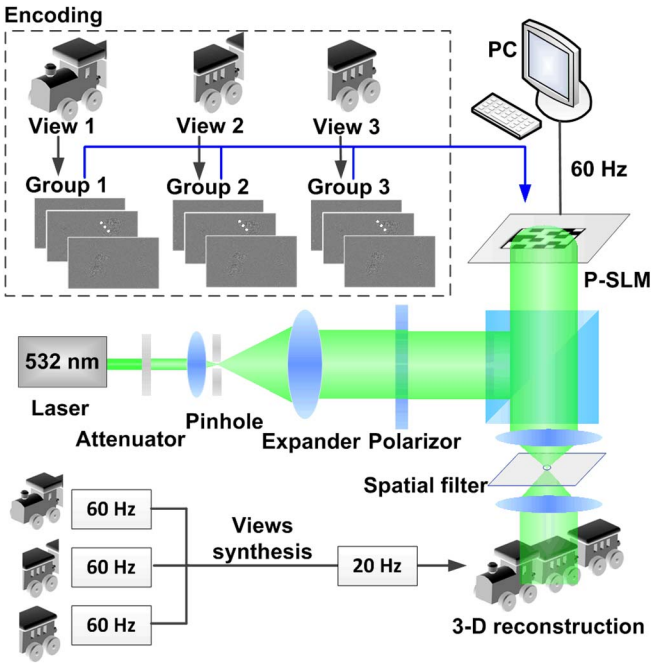

Fig. 4. Experimental setup of the proposed time-division multiplexing holographic 3-D display.

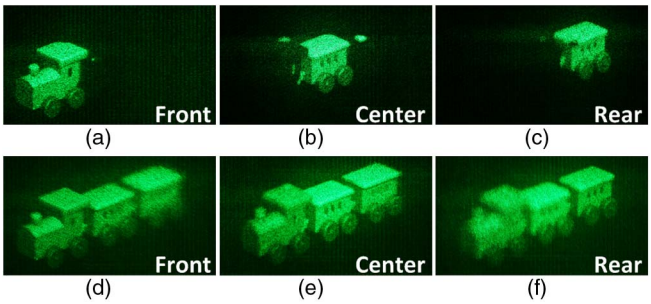

Fig. 5. (a), (b), and (c) are the reconstructions of group-CGH 1, 2, 3, respectively, with the exposure time of 1/60 s. (d), (e), and (f) are the reconstructions when focusing on the front, center, and rear parts of the train, respectively, with the exposure time of 1/20 s.

frame. The depth range of each reconstruction zone is about 6.67 mm, and the overall depth of the reconstructed train is 20 mm.

Figure 4 is the experimental setup of the proposed time-division multiplexing holographic 3-D display. A solid-state laser at a wavelength of 532 nm is used as the light source. PLUTO phase-only SLM (HOLOEYE Photonics AG), a reflective liquid crystal on silicon (LCOS) micro displayer with pixel number 1920 × 1080 and pixel pitch 8 μm, is utilized to load CGHs. Each pixel modulates the phase of the incident light and reflects the modulated light. The optical field is then filtered by a spatial filter through a 4-f system, which is formed by two Fourier lenses. With the help of the spatial filter, the zero-order interruption is eliminated[26]. Reconstructed images can be viewed directly along the optical axis.

The optical reconstructions of the train are shown in Fig. 5. Each group-CGH reconstructs one frame of the 3-D image. Figures 5(a)–5(c) are captured sequentially within the exposure time of 1/60 s and focusing on the front, center, and rear part of the train, respectively. Three different frames are obtained separately. Then, a whole 3-D image of the train is captured within the exposure time of 1/20 s. This time-division multiplexing method makes full use of the high refresh rate of the SLM device, which can fuse the reconstruction images of three group-CGHs into a complete 3-D scene. The optical reconstruction results of the train as a whole are shown in Figs. 5(d)–5(f), which are focused at 210, 220, and 230 mm, respectively. The 3-D train is reconstructed successfully, which verifies that the method of time-division multiplexing holographic display is feasible.

To further demonstrate the effectiveness of the proposed time-division multiplexing method, a 2-D image is used for analyzing the image quality due to the lack of quantitative methods of evaluating the 3-D images. The original image (microscopic image of pollen grains) shown in Fig. 6(a) is located at 250 mm behind the hologram plane. The reconstruction of one phase CGH using the angular-spectrum algorithm is shown in Fig. 6(b), and the signal-to-noise ratio (SNR) of the reconstructed image

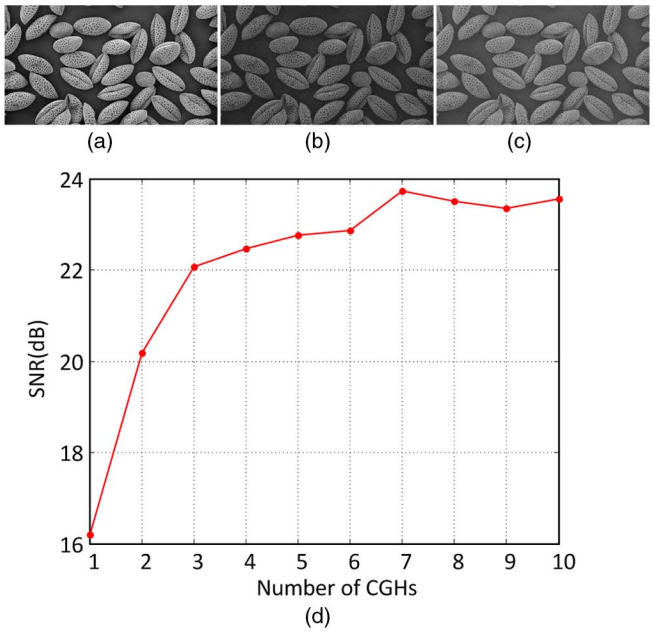

Fig. 6. Numerical reconstructions of the microscopic image of pollen grains. (a) The original image, (b) the reconstructed image with one single CGH, (c) the reconstructed image with 7 group-CGHs, and (d) the SNR curve of the reconstructed images with the number of time-division multiplexed CGHs.

compared to the original image is 16.2 dB. To implement time-division multiplexing processing, the original image is segmented into different numbers of subimages, with the interlaced modes for calculating the corresponding number of group-CGHs. The segmentation is implemented according to the row indexes of the image. Each group-CGH is generated by a set of nonadjacent rows of the original image. Figure 6(c) shows the reconstructed image using 7 group-CGHs with the SNR 23.7 dB. Figure 6(d) shows the SNR curve of the reconstructed images with the number of group-CGH in usage. It can be seen that the SNR is maintained above 22 dB when using more than 3 group-CGHs for reconstructing. The improvement of the reconstruction quality would be more obvious if a complex 3-D scene is used for calculating the CGHs.

The number of layers that can be added in a single reconstruction depends on the dynamic range of the SLM and the digitization noise. The cross talk between the adjacent reconstructed layers affects the image quality of the reconstruction. The minimum adjacent distance could be evaluated by the reconstructions. As shown in Figs. 7(a)–7(c), three reconstructed images are shown when the observation depths are $d = 219.5$, 220, and 220.5 mm, respectively. The reconstructions can be observed even off the designed layer depth $d = 220$ mm. The MSE vs. distance curve is presented in Fig. 7(d). It is shown that the MSE is very high beyond the range from 219.5 to 220.5 mm. Thus, the spatial sensitivity of the layer is about 1 mm. When the distance interval between the layers is smaller than 1 mm, the cross talk will affect the reconstructed 3-D images.

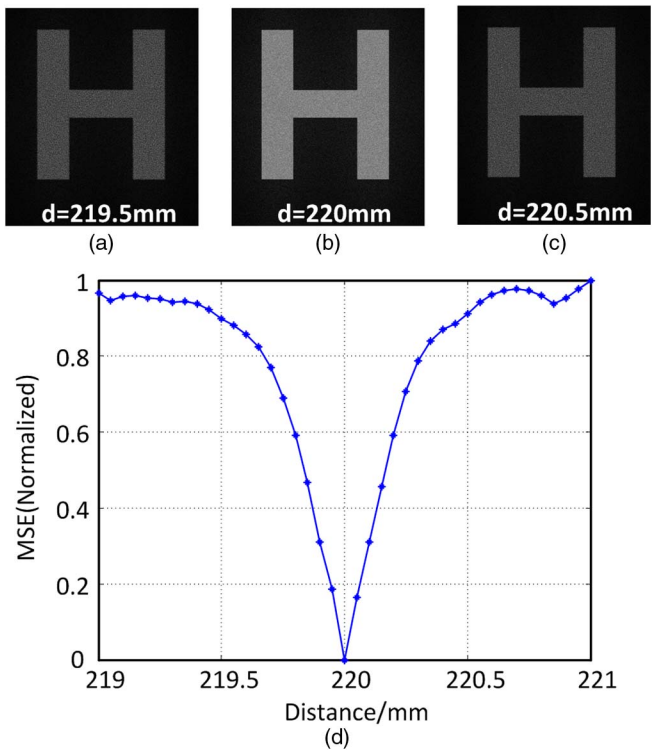

Fig. 7. Reconstructed images (a), (b), (c) are at the distances of 219.5, 220, and 220.5 mm, respectively. (d) The normalized MSE varies with the distance shift at the depth of 220 mm.

The limited SBP of the SLM is the current bottleneck of the holographic display system. In this work, with the time-division multiplexing method, we successfully demonstrate the improved holographic display using a phase-only SLM at a fresh rate of 60 Hz. A 3-D scene is sliced into multiple layers to generate a serial of grouped CGHs for time-division multiplexing. By using high-speed SLM, the quality of the optical reconstruction from multiplexed group-CGHs is better than that of one single CGH. The angular-spectrum algorithm can provide a fast and rigorous computation of the wavefront propagation from the layers to the hologram without any paraxial approximation. This time-division multiplexing method can also be combined with other available spatial multiplexing methods to further enhance the SBP of the holographic display system.

This work was supported by the National Basic Research Program of China (No. 2013CB328801) and the National Natural Science Foundation of China (Nos. 61505095 and 61205013).

References

1. S. A. Benton and V. M. Bove, *Holographic Imaging* (John Wiley and Sons, 2007).
2. H. Zhang, Y. Zhao, L. Cao, and G. Jin, Chin. Opt. Lett. **12**, 060002 (2014).
3. F. Yara, H. Kang, and L. Onural, J. Display Technol. **6**, 443 (2010).
4. P. St. Hilaire, S. A. Benton, M. Lucente, M. L. Jepsen, J. Kollin, H. Yoshikawa, and J. Underkoffler, Proc. SPIE **1212**, 174 (1990).
5. P. St. Hilaire, S. A. Benton, and M. Lucente, J. Opt. Soc. Am. **9**, 1969 (1992).
6. D. E. Smalley, Q. Y. Smithwick, V. M. Bove, Jr., J. Barabas, and S. Jolly, Nature **498**, 313 (2013).
7. C. W. Slinger, C. D. Cameron, S. D. Coomber, R. J. Miller, D. A. Payne, A. P. Smith, M. G. Smith, M. Stanley, and P. J. Watson, Proc. SPIE **5290**, 27 (2004).
8. J. Hahn, H. Kim, Y. Lim, G. Park, and B. Lee, Opt. Express **16**, 12372 (2008).
9. F. Yaraş, H. Kang, and L. Onural, Opt. Express **19**, 9147 (2011).
10. H. Sasaki, K. Yamamoto, K. Wakunami, Y. Ichihashi, R. Oi, and T. Senoh, Sci. Rep. **4**, 6177 (2014).
11. Y. Takaki and M. Yokouchi, Opt. Express **19**, 7567 (2011).
12. Y. Takaki and K. Fujii, Opt. Express **22**, 24713 (2014).
13. T. Inoue and Y. Takaki, Opt. Express **23**, 6533 (2015).
14. Y. Sando, D. Barada, and T. Yatagai, Opt. Lett. **39**, 5555 (2014).
15. M. Lucente, J. Electronic Imaging **2**, 28 (1993).
16. S. Kim and E. Kim, Appl. Opt. **47**, D55 (2008).
17. Y. Ogihara and Y. Sakamoto, Appl. Opt. **54**, A76 (2015).
18. K. Matsushima, Appl. Opt. **44**, 4607 (2005).
19. H. Kim, J. Hahn, and B. Lee, Appl. Opt. **47**, D117 (2008).
20. L. Ahrenberg, P. Benzie, M. Magnor, and J. Watson, Appl. Opt. **47**, 1567 (2008).
21. J. Chen, D. Chu, and Q. Smithwick, J. Electronic Imaging **23**, 023016 (2014).
22. J. Chen and D. Chu, Opt. Express **23**, 18143 (2015).
23. M. Bayraktar and M. Özcan, Appl. Opt. **49**, 4647 (2010).
24. Y. Zhao, L. Cao, H. Zhang, D. Kong, and G. Jin, Opt. Express **23**, 25440 (2015).
25. J. W. Goodman, *Introduction to Fourier Optics*, 2nd ed. (McGraw-Hill, 1996).
26. H. Zhang, Q. Tan, and G. Jin, Opt. Eng. **51**, 075801 (2012).